TOWARD THE CFD SIMULATION OF SIROCCO FANS: FROM SELECTING A TURBULENCE MODEL TO THE ROLE OF CELL SHAPES

Manoochehr DARVISH, Stefan FRANK

University of Applied Sciences HTW Berlin,
Wilhelminenhofstr. 75A, 12459 Berlin, Germany

SUMMARY

This paper presents a comprehensive study on the CFD simulation of a radial fan with forward curved blades emphasizing on turbulence models and unstructured grids. Three of the most widely used turbulence models i.e. Realizable k-ε, SST k-ω and Spalart-Allmaras are validated with the available experimental results. The model performance comparison is based on the characteristic curves and the velocity fields obtained from each model. The other part of the study concentrates on the unstructured grids, addressing the influence of cell shapes on the accuracy of the results. The verification efforts in this part focus on predicting the characteristic curves.

INTRODUCTION

Radial fans with forward curved blades (also known as Sirocco fans or squirrel cage fans) are capable of delivering higher flow rates and also producing higher static pressure than other centrifugal fans of the same size and speed [1, 3]. Sirocco fans are mainly used in the automotive industry and in heating, ventilation and air conditioning (HVAC) applications.

Due to the complexity of the flow in Sirocco fans and the wide range of their applications, they have been the subject of many research studies; each trying to gain a better understanding of the flow field, address and overcome the deficiencies of this type of fan.

In the previous studies, the investigations of the flow field inside the Sirocco fans are conducted using different methods, such as five hole pressure probe [5], hot wire probe [6], Particle Tracking Velocimetry PTV [7, 8], Particle Image Velocimetry PIV [9], Laser Doppler Anemometry [10] and Spark Tracing Method [11]. The results achieved by these methods helped to gain insights into the characteristics of the flow in Sirocco fans. In addition to the experimental studies, Computational Fluid Dynamics CFD has been used by many researchers as an effective tool. The aim of these CFD simulations were mainly testing the reliability of the CFD codes through the comparison of numerical results against the experimental data [12, 13] and/or improving the performance of the fan through obtaining the optimized shape of the impeller blades [14] and volute [15], improving

slip factor models [16] and reducing the generated noise [17]. Structured grid and the *k-ε* turbulence model is a common combination that can be found in a series of the previous works (refer to [14, 15, 16, 18]). However, the flow field comparisons are limited to the overview of the experimental data beside the captured CFD results.

In this study, the role of cell shapes and the influence of the turbulence models are verified. The numerical data obtained from models are compared against the experimental results. Comparisons of the captured velocity fields are conducted precisely in 2D and 3D against the experimental data for different turbulence models. Moreover, for testing the accuracy of the steady state simulations and addressing their deficiency in the throttle range, unsteady simulations are performed, and the applicability range of each method is identified on the characteristic curve of the fan.

Flow inside Sirocco fans

The flow inside Sirocco fans can be referred to as fully 3D, turbulent and unsteady. The complexity of the flow stems from the fact that there are inevitable flow separation zones in the fan. Although some of the separation zones are relatively small, they are large enough to reduce the performance and decrease the efficiency.
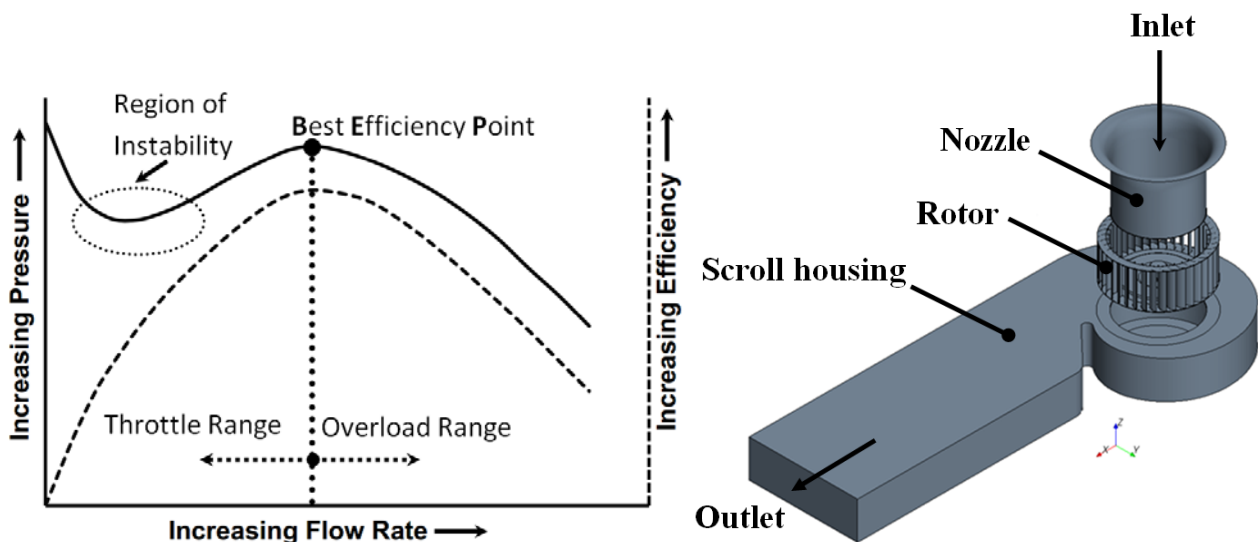

Figure 1 : Schematic performance curve of a Sirocco fan (left); Exploded view of the fan model (Right)

One of the most considerable flow separations occurs in the blade passages, which makes the blades stalled even at the Best Efficiency Point BEP [1] (see Figure 2). An extensive flow recirculation zone can develop after the volute tongue (Figure 2). This separation zone is highly expected in the overload range.

Another flow separation zone can also be formed near the cut-off (not shown), which makes a re-entrant flow through the rotor [5]. This reverse flow is most prevalent in the throttle range and can be inhibited by modifying the design variables [31].

The next separation zone develops near the inlet nozzle. This flow separation leads to the formation of an inactive zone in the rotor that can grow up to one third of the rotor width [5]. The secondary flow pattern (or secondary vortex flow) [30], which develops within the volute and distorts the primary flow, is the consequence of the near inlet separation and the inactive zone [19] (Figure 3).
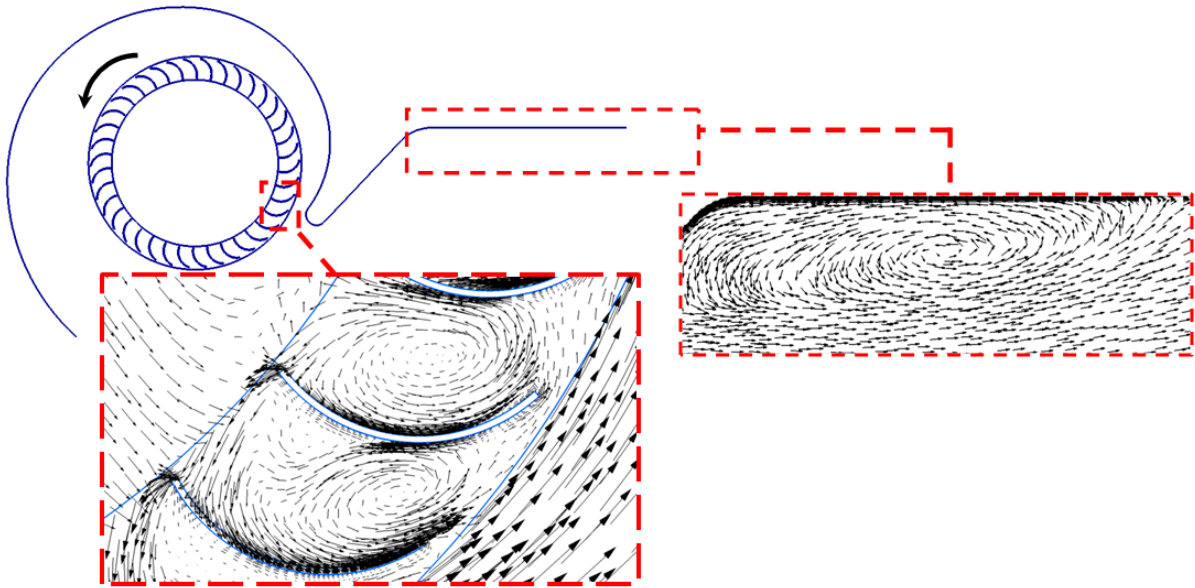
Figure 2: Flow separation between impeller blades and after the volute tongue in a Sirocco fan

Due to the complexity of the flow, design calculations of Sirocco fans cannot be as accurate as for other types of fans; in fact there is a high level of uncertainty associated with the flow rate and pressure requirement for calculating the dimensions and obtaining a satisfactory prototype of this kind of fan. In this perspective CFD can be used as a design and analysis tool to improve the performance through providing detailed information about the characteristics of Sirocco fans.
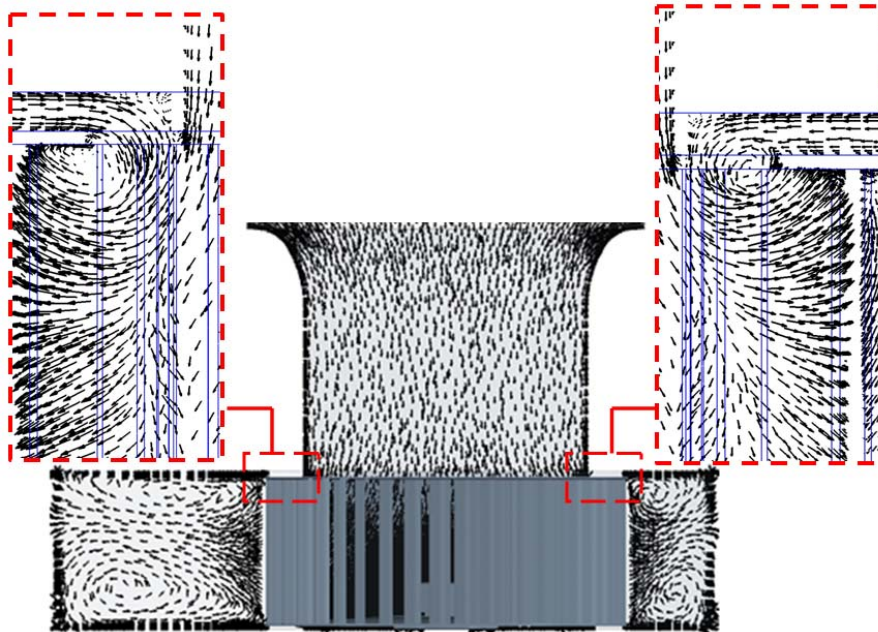

Figure 3: Illustration of the secondary flow in the scroll and the inactive zone near the inlet

EXPERIMENTAL SETUP

The fan under consideration is a Sirocco fan with 38 small forward curved blades and an outer diameter of 200 mm. It is mounted in a scroll-type casing that collects the flow and discharges it through a rectangular outlet (see Figure 1).

The fan is installed on a chamber test rig in accordance with ISO 5801 / DIN 24163. The performance data such as pressure rise, shaft power and static efficiency are collected for a range of flow rates at the rotating speed of n = 1000 rpm.

Furthermore, Particle Image Velocimetry (PIV) technique is used to measure the velocity fields. 2D velocity fields are captured by means of one camera on a plane which consists of approximately 13000 points, and 3D velocity fields are captured by two cameras on a smaller plane which consists of 6000 points (see Figure 4). These points are also used in the post-processing of the CFD simulations, to capture the velocity fields on the same grid as the experimental measurements. This results in an accurate point to point velocity field comparison between PIV and CFD. Further information about the experimental part of the study and PIV measurements can be found in [31].

Table 1 : Technical specifications of the Sirocco fan modeled in the study

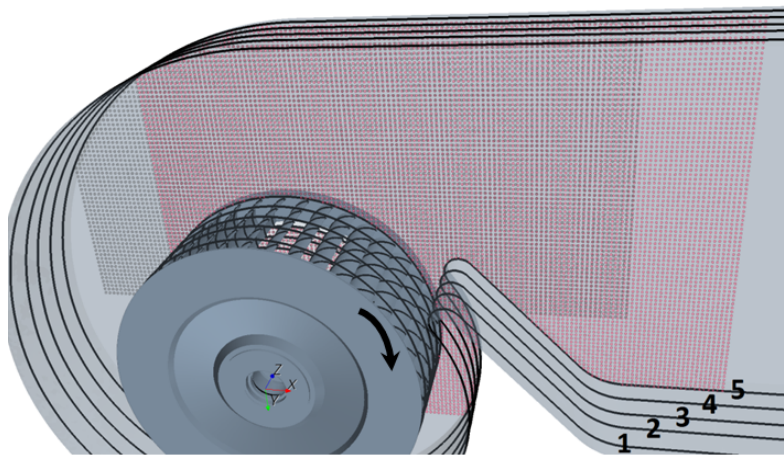| Parameter		Dimension
Rotor	Fan wheel outer diameter | inner diameter | width	200 mm | 160 mm | 82 mm
	Blade width × length × thickness	80 mm × 25 mm × 0.6 mm
	Blade curvature	15 mm
	Inlet blade angle | Outlet blade angle	~ 80° | ~ 170°
	Number of blades	38
Stator	Volute width	87 mm
	Volute opening angle | tongue angle	7° | 23°
	Volute tongue radius	10 mm

Figure 4: PIV planes, used for experimental measurements; velocity fields captured on plane 5 are used in this study

NUMERICAL SETUP

The numerical part of the study is performed using Star-CCM+, a commercially available CFD package [29]. The first part of the numerical simulations highlights the role of cell shapes in the accuracy of the results, with the second part addressing the performance of different turbulence models.

Numerical simulations are performed in the steady-state mode by using Moving Reference Frame (MRF) approach (also called "frozen rotor" in some literatures). Applying MRF to a region will not change the position of the cell vertices, but generates a constant grid flux in the appropriate conservation equations. MRF can be used for an approximate analysis of a constant motion in steady-state mode, which leads to a solution representing the time-averaged behavior of the flow [2, 29]. Apart from MRF simulations, part of this study is devoted to unsteady simulations using Rigid

Body Motion (RBM) approach. Applying RBM to a region will rigidly move the mesh vertices of a region. Despite the more accurate results that can be obtained from RBM, this approach is not favored for engineering purposes, due to the fact that movement of the mesh vertices makes this approach very time consuming, especially when the model contains numerous cells and vertices.

CFD Simulations are carried out using a workstation equipped with an Intel Core i7 CPU (2.8 GHz) and 8 GB RAM.

Mesh configurations

Structured grid is the most widely used grid type in turbomachinery simulations. Despite all the advantages of structured grids, there is a critical disadvantage concerning their inflexibility to complex geometries. This imposes a large amount of effort to the mesh generation procedure and makes it very time consuming. On the other hand unstructured grid generators are capable of discretizing complex geometries with less effort and minimum user interaction. The collection of the cell shapes that are available for unstructured mesh generators provides a great flexibility in the treatment of any kind of geometry. Nevertheless, the lack of an explicit structure in the mesh necessitates a compensating data structure in the solver, which demands more powerful computing resources. The point mentioned is the prominent disadvantage of unstructured grids [2].

In order to evaluate the performance of the unstructured grids in the simulation of Sirocco fans, three unstructured grids are generated using Star-CCM+. Concerning the amount of cells, the goal is to create unstructured grids that are comparable to the structured grid used in this study. The structured grid is generated by means of the blocking approach of ANSYS ICEM. Sensitivity study on the structured grid showed that the grid independency can be achieved by a model which is consisted of about 4 million nodes (approximately 3.5 million cells) [9]. Furthermore, the mesh sensitivity study performed for unstructured grids showed that 60% refinement of a mesh with approximately 4 million cells, leads to only 1% change in the simulation reports (i.e. static pressure and torque). Therefore, unstructured grids are generated by using identical settings in the mesh generators. A high quality resolved mesh is provided by the mesh generators on the important boundaries e.g. averaged dimensionless wall distance $y^+ < 2$ around the blades surface.

Table 2 presents an overview of the mesh configurations employed in this study. According to this table, the efficiency of each model can also be distinguished.
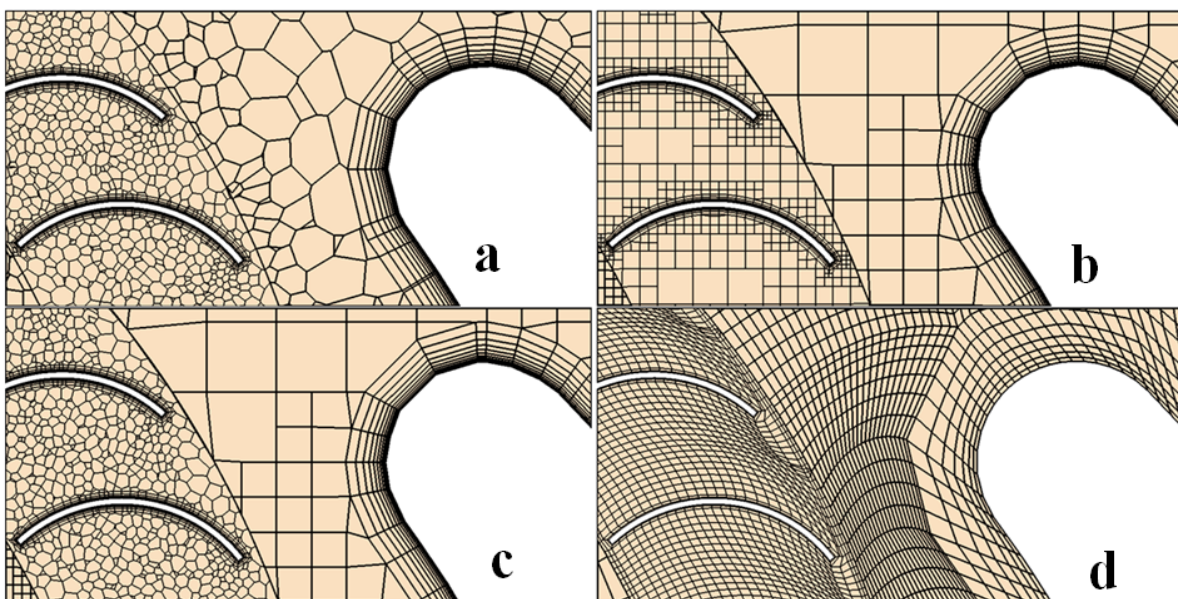

Figure 5 : Four mesh configurations used in this study; a) polyhedral cells b) trimmed hexahedral cells c) combination of polyhedral and trimmed cells d) structured hexahedral cells

Table 2 : Overview of the generated mesh configurations

		Polyhedral	Trimmer	Polyhedral-Trimmer	Structured
Number of Cells (in millions)	**Total**	4.2	6.1	4.0	3.7
	Rotor	2.6	4.8	2.7	2.4
	Stator	1.6	1.3	1.3	1.3
Number of vertices | Faces		15.6 | 21.9	7.5 | 18.2	10.4 | 16.8	4.3 | 10.8
Mesh generation time		1-2 hours			2-3 days

Turbulence models

In the interest of evaluating the performance of RANS turbulence models in the simulation of Sirocco fans and to investigate the sensitivity of these simulations to turbulence models, CFD simulations are performed by using three of the most popular turbulence models:

The Spalart-Allmaras model [22] is the most widely used one-equation turbulence model, which is based on a transport equation for the turbulent viscosity. This is in contrast to many of the early one-equation models that solve an equation for the transport of turbulent kinetic energy and requires an algebraic prescription of a length scale [29]. One of the favorable features of the Spalart-Allmaras is that it is a local model. It means that the equation at one point does not depend on the solution at other points [2]. In this study, the Spalart-Allmaras model is used in its standard form, which is designed to be applied without wall functions [29].

Realizable k-ε [23] is a two-equation model, which is one of the most successful modifications of the k-ε model. This model contains a new transport equation for the turbulent dissipation rate. In comparison with the standard k-ε model, Realizable k-ε provides a more accurate prediction of the characteristics of rotational flows, boundary layers subjected to strong pressure gradients, separated flows and the streams in which developed secondary flows exist [24]. In this study, Realizable k-ε is used with the two layer method [25] that enables it to be applied in the viscous sublayer. In this approach the values of dissipation rate specified in the near-wall layer are blended smoothly with the values computed from solving the transport equation far from the wall [29].

The Shear-Stress-Transport SST k-ω model [21] is a two-equation model, which combines several desirable elements of other two equation models [26]. The first major feature of SST model is the blending function which enables it to switch the model coefficients [24, 26]. As a result, SST k-ω uses the standard k-ω model near the solid walls and standard k-ε model near boundary layer edges and in free shear layers [29]. The next feature is the modification of the eddy viscosity function to improve the prediction of flows with strong adverse pressure gradients and flow separation [26, 27]. Unlike the standard model, SST model is not sensitive to the free stream and inlet conditions [29].

The turbulence models are used with the all-y^+ wall treatment in this study. This is a hybrid treatment that attempts to emulate the high-y^+ wall treatment for coarse meshes and low-y^+ wall treatment for fine meshes [29].

RESULTS AND DISCUSSION

In order to increase the accuracy of the results and investigate the interaction between the fan blades and volute tongue, simulations are performed for different rotor positions, so that after each simulation, the fan wheel is manually rotated for 1°, and the simulation is repeated for the new position of the fan. The averaged results are calculated after 9° rotation of the fan, which is approximately equal to the angular distance between two adjacent blades. Comparison of the simulation results showed that there is a negligible difference of 0.5% between the result of one

rotor position and the averaged results of 9 rotor positions. Therefore, it can be concluded that the simulation results (e.g. pressure rise, power etc.) are independent of the position of the blades. Hence the steady simulations are performed for one rotor position in this study.

Characteristic curves obtained from CFD simulations of different grids are shown in Figures 6 and 7. The simulations are performed in steady mode, using SST k-ω turbulence model. As shown below, the obtained results correctly follow the trend of the experimental data. Especially in the overload-range, where the performance of the fan is stable, there is good agreement between CFD and experimental results.
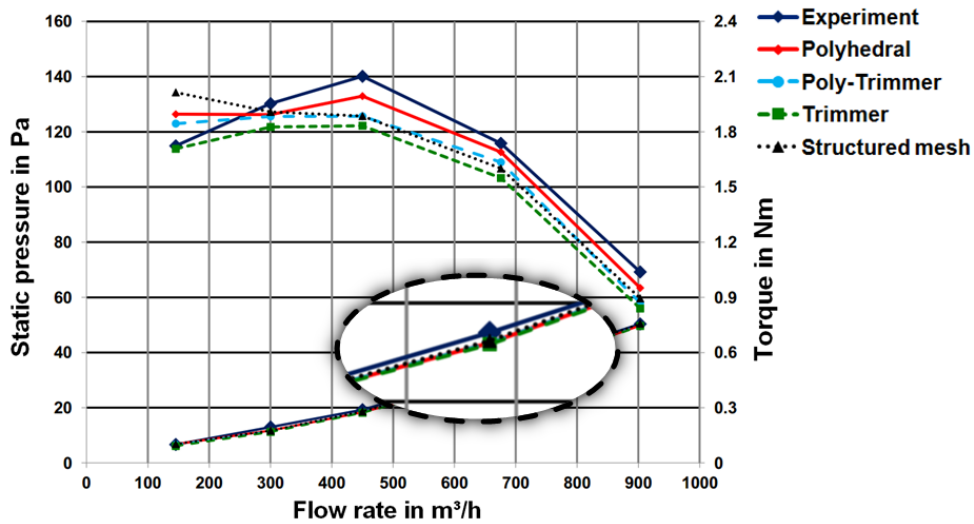
Figure 6: Comparison of the characteristic curves obtained by different grids

According to Figure 6, results obtained by the polyhedral mesh model have the least amount of deviation from the experimental results (approximately 5% in static pressure and torque at BEP).
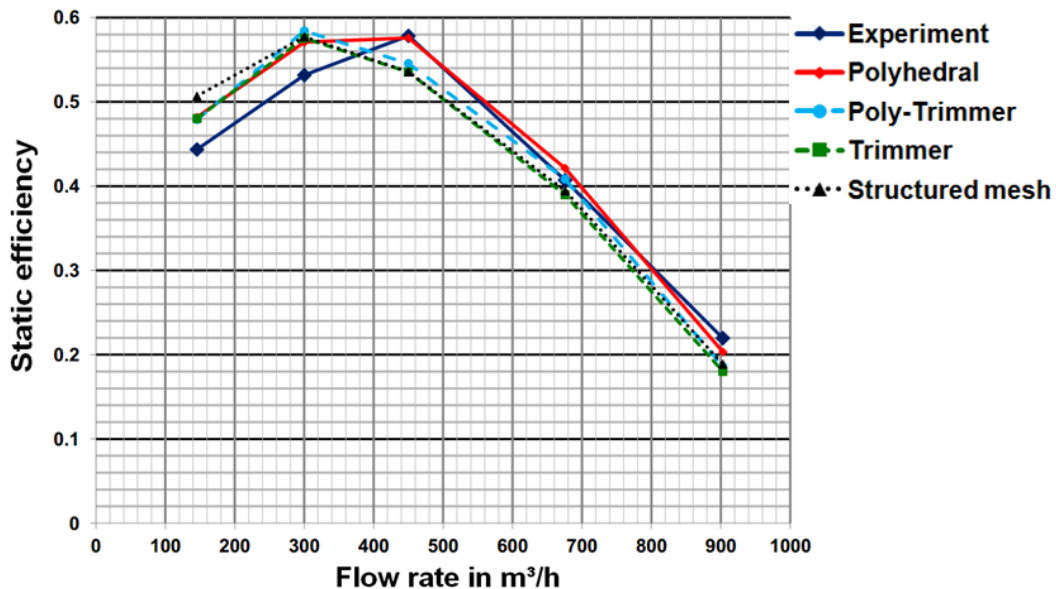

Figure 7: Static efficiency vs. Flow rate obtained by different grids; Altogether, the most accurate results are obtained by Polyhedral mesh

For all turbulence models, torque convergence starts after 100 iterations, whereas the convergence of the pressure monitor starts after 300 iterations. It is necessary to continue the simulations up to 1000 iterations to get fully converged velocity fields. However, there is a high level of uncertainty associated with the convergence in a part of the throttle range (flow rates less than 300 m³/h). Concerning the solver elapsed time, the simulation time of poly-trimmer model is almost equal to

the structured model and approximately 20% faster than polyhedral model, whereas trimmed mesh is 6% slower than polyhedral model.

According to the characteristic curves obtained by performing CFD simulations using polyhedral mesh with different turbulence models (Figures 8 and 9), it is apparent that all turbulence models predict the trend of the experimental data and the peak pressure point correctly. However SST k-ω results are in better agreement with experimental data. There are negligible differences between the torque results obtained from different turbulence models; In fact the curves are superimposed at most of the flow rates.
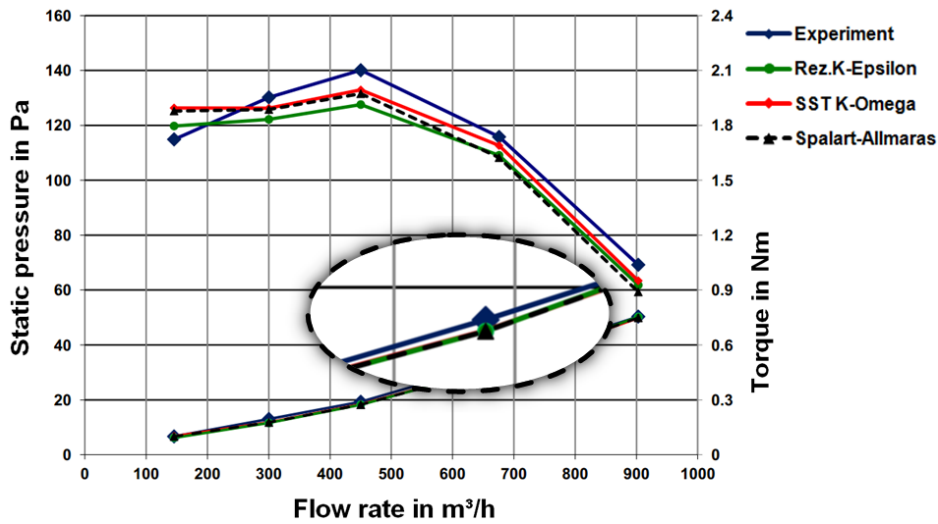

Figure 8: Comparison of characteristic curves obtained by different turbulence models; the most accurate results are obtained from SST k-ω model
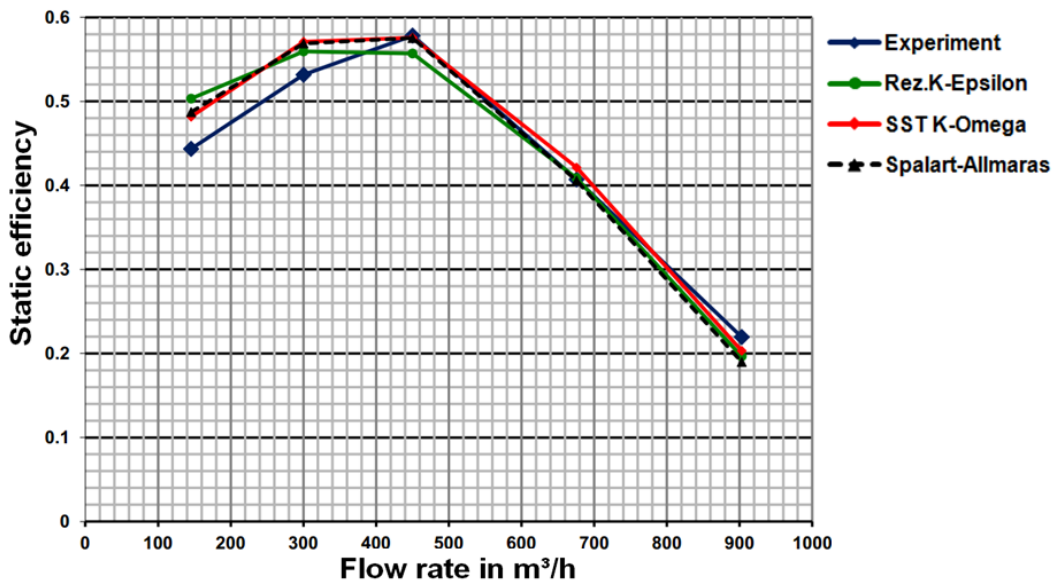

Figure 9: Static efficiency vs. Flow rate predicted by different turbulence models

The simulation with Spalart-Allmaras model is 10% faster than the other two turbulence models. The difference between Realizable k-ε and SST k-ω is negligible in this comparison. For all turbulence models, torque convergence starts after 100 iterations, whereas the pressure convergence starts after 200 iterations. However, it is necessary to continue the simulations up to 1000 iterations to get converged velocity fields.

Figure 10 represents the PIV captured velocity fields at the Best Efficiency Point (i.e. flow rate of 450 m³/h and n = 1000 rpm). The results belong to the last PIV plane (plane number 5 in Figure 4).
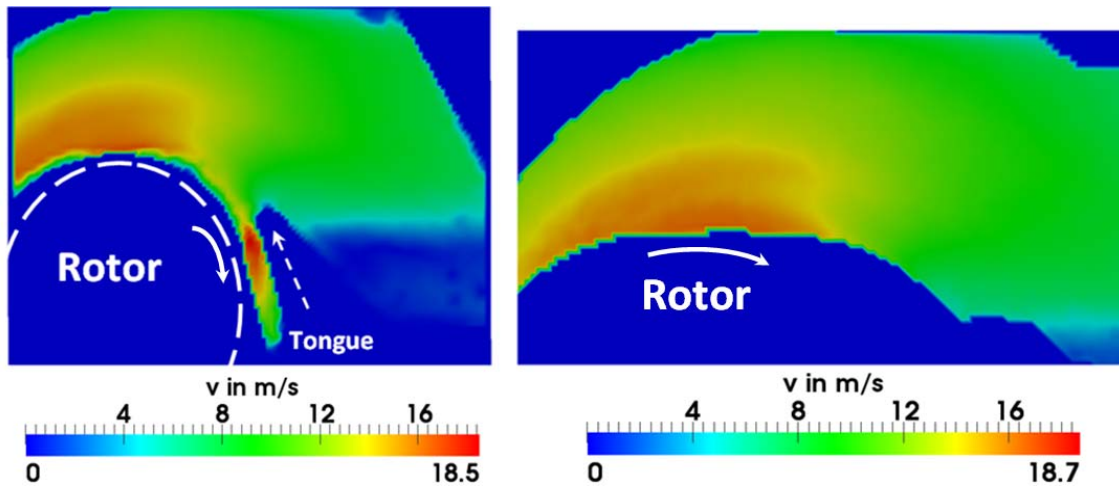
Figure 10: 2D (Left) and 3D (Right) velocity fields captured by PIV measurements at BEP (450 m³/h)

Figure 11 illustrates the absolute difference of the velocity fields captured for different turbulence models. According to this figure, the models which have the least deviation from the experimental characteristic curves have more accurate velocity fields.
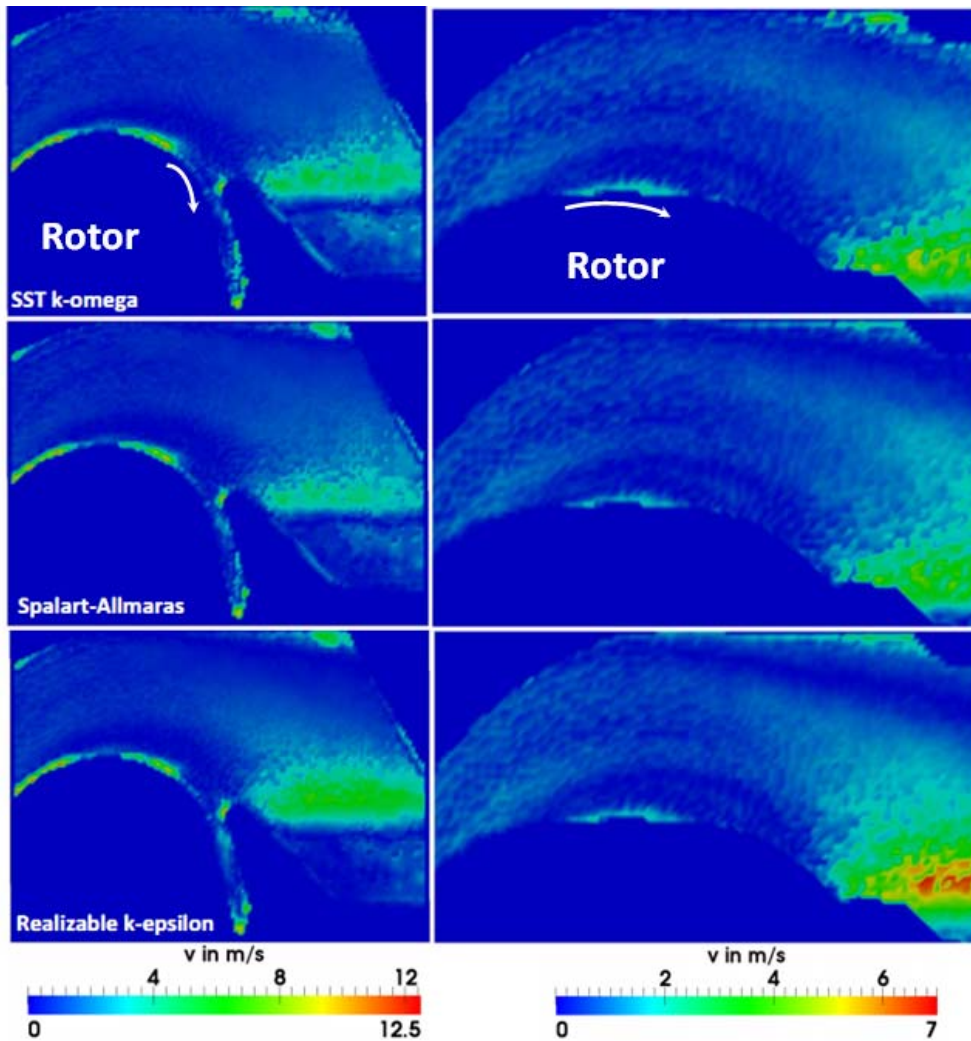

Figure 11: Absolute velocity field differences between PIV and CFD for different turbulence models; 2D comparisons on the left and 3D velocity field comparisons on the right

In Figure 11 there are mainly two parts where discrepancies between PIV and CFD results can be found. The first part includes the boarders of the plane used for the PIV measurements, which are

close to either the volute or the fan-wheel. In these areas, due to the reflection of the laser lights, it is not possible to reliably capture PIV data. The next part is the area downstream of the volute tongue, in which - besides the experimental uncertainties - steady-state results might be the source of discrepancies. This claim is based on the comparisons of the steady (MRF) and unsteady (RBM) results in Figure 14.

Figure 12 represents a comparison between the MRF (steady) and RBM (unsteady) characteristic curves obtained by employing SST *k-ω* and polyhedral models.
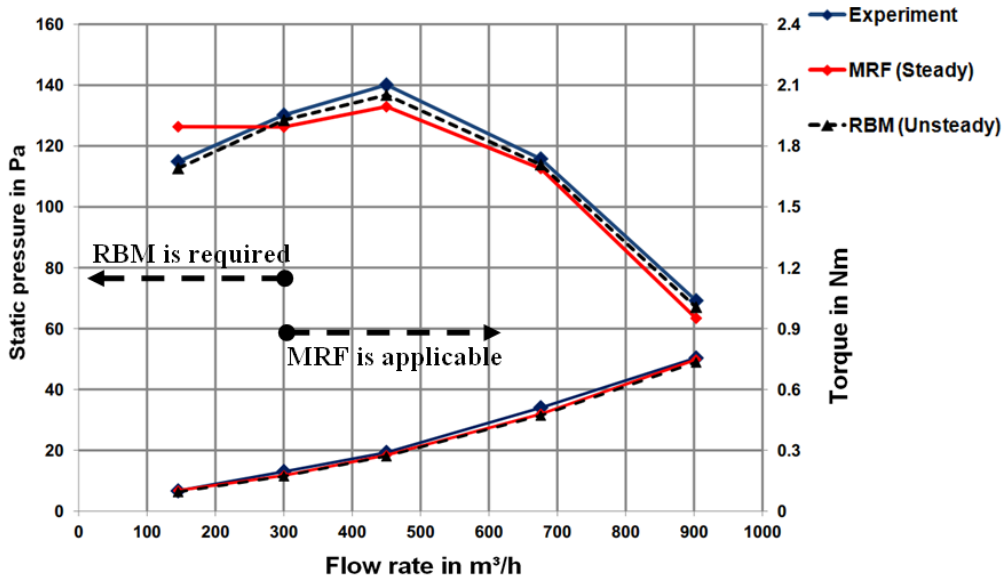

Figure 12: Characteristic curves obtained by MRF (steady) and RBM (unsteady) simulations

Apparently RBM method is able to predict the trend of the experimental curve for the whole operating range of the flow rates, unlike the MRF method which cannot predict the trend of the experimental curve in the throttle range. Although the deviation of MRF results are well within 10%, more accurate results can be obtained by performing unsteady simulations (RBM approach).

The results reported as the final unsteady results are the averaged results of the two last revolutions of the fan, from where the monitor curves were fully converged (see Figure 13). It took approximately 30 hours to simulate one complete revolution of the fan (with 10 inner iterations and 1.5° rotation per time-step). For obtaining converged velocity fields, it is necessary to continue the simulations for at least five revolutions. Whereas, it took only 8 hours to achieve converged results (for each operating point) by using MRF method.
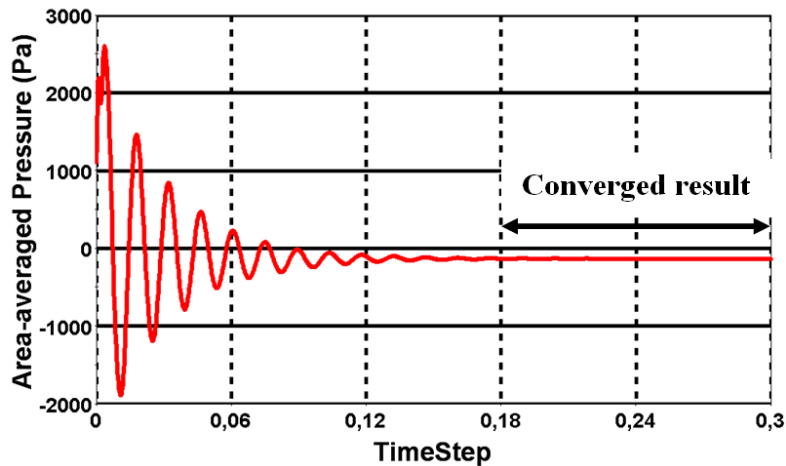

Figure 13 : Inlet pressure monitor curve obtained from unsteady simulation at BEP; The averaged value reported as the final result is calculated from the time step where the monitor curve starts to converge (time step=0,18 s to 0,3 s)

Considering the velocity field comparisons made between CFD and PIV results (Figure 14), a better agreement between the unsteady velocity fields and PIV results can be verified. Especially in the area downstream of the volute tongue (as already mentioned as one of the incompatible areas) more accurate results are obtained by unsteady simulations. Nevertheless it is apparent that there is a good similarity between the MRF and RBM results in most parts.
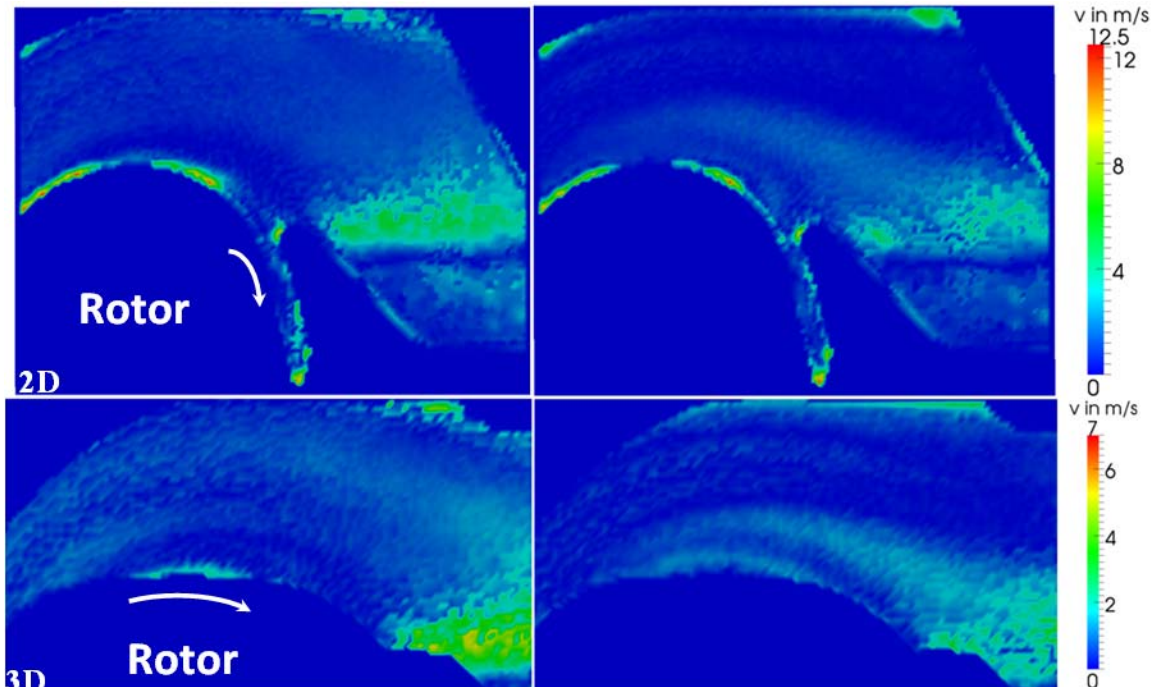

Figure 14: Absolute velocity field comparisons of steady (Left) and unsteady (Right) simulations with PIV data

CONCLUSIONS

Based on the validation studies, it can be concluded that unstructured grids can be used effectively for the CFD simulation of Sirocco fans, and a considerable amount of mesh generation time can be saved by using them. Among the mesh configurations investigated in this study, results obtained from polyhedral model have the least deviation from the experimental curves.

According to the characteristic curves and velocity fields obtained by different turbulence models, it is concluded that SST k-ω is the best model that can be used for the simulation of Sirocco fans. The correlation between the CFD predictions using MRF approach and the experimental results is close enough to support the use of this approach as a tool for simulating Sirocco fans. However, for obtaining more accurate results in the throttle range, it is recommended to perform unsteady simulations by using RBM approach.

ACKNOWLEDGMENT

BIBLIOGRAPHY

[1] F. P. Bleier − *Fan handbook:selection,application and design*, McGraw-Hill, **1997**
[2] J. Balzek − *Computational Fluid Dynamics:Principles and applications,* Elsevier, **2001**
[3] J. F. Kreider − *Handbook of heating,ventilation and air conditioning*, CRC Press, **2001**
[4] B. Eck − *Design and Operation of Centrifugal, Axial-Flow, and Cross-Flow Fans*, Pergamon Press, **1973**

[5] R. J. Kind, M. G. Tobin − Flow *in a Centrifugal Fan of the Squirrel-Cage Type*, ASME Journal of Turbomachinery, Vol. 112, **1990**

[6] D. Raj, W. B. Swim − *Measurements of the mean flow velocity and velocity fluctuations at the exit of an FC centrifugal fan rotor*, ASME Journal of Engineering for power, **1981**

[7] G. R. Denger, M. W. Mcbride, G. C. Lauchle − *An Experimental Evaluation of the Internal Flow Field of an Automotive Heating, Ventilating and Air Conditioning System*, TR 90-011, Penn State University, **1990**

[8] H. Tsurusaki, Y. Tsujimoto, Y. Yoshida, K. Kitagawa − *Visualization Measurement and Numerical Analysis of Internal Flow in Cross-Flow Fan*, Journal of Fluids engineering, Vol.119, **1997**

[9] A. Stuchlik, S. Frank, P.-U. Thamsen − *Performance investigation of Sirocco fans by means of Computational fluid dynamics*, ISROMAC-13, Hawaii/USA, **2010**

[10] N. Montazerin, A. Damangir, H. Mirzaie − *Inlet induced flow in squirrel-cage fans*, Journal of Power and Energy Vol. 214, **2000**

[11] S. Kadota, K. Kawaguchi, M. Suzuki, K. Matusi, K. Kikuyama − *Experimental study on low- noise multiblade fan (1st Report, visualization of 3D Flow between Blades)*, JSME No.93-0739, **1994**

[12] S. V. Suárez, R. B. Tajadura, J. G. Pérez − *Numerical Simulation of the Unsteady Flow Patterns in a Small Squirrel-Cage Fan*, ASME Joint U.S.-European Fluids Engineering Summer Meeting, **2006**

[13] M. Younsi, F. Bakir, S. Kouidri, R. Rey − *Numerical and experimental study of unsteady flow in a centrifugal fan*, Proc.IMechE Vol.221 Part A: J. Power and Energy, **2007**

[14] K. -Y. Kim, S. J. Seo − *Application of numerical optimization technique to design of forward-curved blades centrifugal fan*, JSME International Journal, Series B, Vol.49, **2006**

[15] S. -Y. Han, J. -S. Maeng − *Shape optimization of cut-off in a multi-blade fan/scroll system using neural network*, International Journal of Heat and Mass Transfer 46, Elsevier **2003**

[16] E. -M. Guo, K. -Y. Kim − *Three dimensional flow analysis and improvement of slip factor model for forward-curved blades centrifugal fan*, The 4th ASME/JSME joint fluids eng. conference, **2003**

[17] Y. Mao, D. Qi, X. Liu, H. Tang − *Numerical prediction of aerodynamic tonal noise radiated from a centrifugal fan*, Journal of Power and Energy Vol. 222, **2008**

[18] Y. Jung, J. Baek − *A numerical study on the unsteady flow behavior and the performance of an automotive sirocco fan*, Journal of mechanical science and technology Vol. 22, **2008**

[19] G. Cau, N. Mandas, N. Manfrida, F. Nurzia − *Measurements of primary and secondary flows in an industrial forward-curved centrifugal fan*, ASME Journal of Fluids Eng. Vol.109, **1987**

[20] D. C. Wilcox − *Turbulence Modeling for CFD*. 1st edition. DCW Industries Inc., **1994**

[21] F. R. Menter − *Two-Equation Eddy-Viscosity Turbulence Models for Engineering Applications*, AIAA Journal, Vol. 32, no. 8., **1994**

[22] P. R. Spalart, S. R. Allmaras − *A one-equation turbulence model for aerodynamic flows*, AIAA Paper 92-0439, **1992**

[23] T.-H. Shih, W. Liou, A. Shabbir, Z. Yang, J. Zhu − *A new k- ε eddy viscosity model for high Reynolds number turbulent flow*, Computer fluids Vol. 24, No.3, Elsevier Science Ltd, **1995**

[24] K. N. Volkov − *Application of a two-layer model of turbulence in calculation of a boundary layer with a pressure gradient*, Journal of Eng. Physics and Thermophysics, Vol. 80, No. 1, **2007**

[25] W. Rodi − *Experience with Two-Layer Models Combining the k-e Model with a One-Equation Model Near the Wall*, 29th Aerospace Sciences Meeting, AIAA 91-0216, **1991**

[26] T. Cebeci − Turbulence *Models and their Application*, Horizons publishing Inc., **2003**

[27] J. E. Bardina, P. G. Huang, T.J. Coakley − *Turbulence Modeling validation, Testing and Development*, NASA Technical Memorandum 110446, April **1997**

[28] U.S. Department of Energy − *Improving fan system performance, a source book for industry* April **2003**

[29] *CD-Adapco User Guide*, Star-CCM+ Version 6.04, **2011**

[30] H. W. Roth − *Optimierung von Trommelläufer-Ventilatoren*, University of Karlsruhe, **1981**

[31] S. Frank, M. Darvish, B. Tietjen, A. Stuchlik − *Design Improvements of Sirocco Type Fans by Means of Computational Fluid Dynamics and Stereoscopic Particle Image Velocimetry*, fan2012 Paper 049, **2012**